JOURNAL OF GEOPHYSICAL RESEARCH, VOL. 115, A02211, doi:10.1029/2009JA014273, 2010

Rayleigh-Taylor type instability in auroral patches

K. Shiokawa,[1] A. Nakajima,[1] A. Ieda,[1] K. Sakaguchi,[1] R. Nomura,[1] T. Aslaksen,[2] M. Greffen,[3] and E. Donovan[3]

Received 19 March 2009; revised 25 September 2009; accepted 2 October 2009; published 26 February 2010.

[1] Based on observations by a high-resolution narrow field-of-view CCD camera, we found small-scale (5–25 km) finger-like structures at the western boundary of auroral patches in images obtained at Gillam (geomagnetic latitude: 65.5°N), Canada, in January 2008. Since shear motion was not observed along the boundary of the patches, we suggest that these structures are formed by macroscopic Rayleigh-Taylor type plasma instability arising in the magnetospheric equatorial plane from the force balancing of the (eastward) magnetic tension force and the (westward) pressure gradient force.

Citation: Shiokawa, K., A. Nakajima, A. Ieda, K. Sakaguchi, R. Nomura, T. Aslaksen, M. Greffen, and E. Donovan (2010), Rayleigh-Taylor type instability in auroral patches, *J. Geophys. Res.*, *115*, A02211, doi:10.1029/2009JA014273.

1. Introduction

[2] The dynamics of auroras is a manifestation of plasma dynamics in the magnetosphere and their coupling with the ionosphere. The discrete auroral arc is a longitudinally extended curtain-like structure, and is generally regarded as a manifestation of shear motion of magnetospheric plasma [e.g., *Haerendel*, 2007]. The shear motion causes vortex-like curls in auroral arcs as a consequence of the Kelvin-Helmholtz instability. Such small-scale structures can be observed using high-resolution auroral TV cameras [e.g., *Hallinan and Davis*, 1970; *Trondsen and Cogger*, 1998; *Sandahl et al.*, 2008]. The high-resolution auroral cameras also reveal Alfven wave structures in multiple arc system [*Semeter and Blixt*, 2006].

[3] At the equatorward boundary of diffuse auroras, large-scale (more than 200 km) wave-like undulations have been often observed by the Defense Meteorological Satellite Program (DMSP) satellites [*Lui et al.*, 1982; *Yamamoto et al.*, 1991], the Thermosphere Ionosphere Mesosphere Energetics and Dynamics (TIMED) satellite [*Zhang et al.*, 2005], the Imager for Magnetopause-to-Aurora Global Exploration (IMAGE) satellite [*Goldstein et al.*, 2005], and ground-based all-sky cameras [*Mendillo et al.*, 1989; *Nishitani et al.*, 1994]. These large-scale undulations in diffuse auroras were also explained by the Kelvin-Helmholtz instability due to the large-scale shear of plasma convection in the inner magnetosphere [e.g., *Kelley*, 1986; *Yamamoto et al.*, 1991, 1993]. The diffuse auroras seen by these satellite imagers usually consist of small-scale patches observed by all-sky cameras from the ground. *Sergienko et al.* [2008] reported a detailed study of fine structures of diffuse aurora using high-resolution ground cameras and the auroral particle measurements by the FAST satellite. However, fine structures in auroral patches have not been well investigated using high-resolution ground auroral cameras.

[4] In this paper, we report small-scale (5–25 km) finger-like structures found at the western boundary of auroral patches, using a high-resolution narrow field-of-view (FoV) camera in the auroral zone. These structures suggest the existence of macroscopic Rayleigh-Taylor type plasma instabilities in the equatorial plane of the magnetosphere.

2. Observation

[5] The observations reported in this paper were made during the THEMIS satellite-ground auroral campaign on 2–16 January 2008 at Gillam (56.4°N, 265.4°E, dipole geomagnetic latitude (MLAT) ~65.5°N) in Canada, when the THEMIS satellite constellation was located in the Canadian longitudinal sector in the equatorial magnetotail [*Shiokawa et al.*, 2009]. Unfortunately the footprints of the THEMIS satellites were not in the FoV of the cameras during the auroral patch events reported in this paper.

[6] Figure 1 is a photograph of the auroral patches taken at Gillam at 1044 UT (0425 LT) on 12 January 2008 by using a color digital camera (NIKON D40). The patches appeared in the northern half of the sky at ~0845 UT after a small substorm (maximum provisional AE index ~ 100 nT) which occurred around 0820 UT. The patches became more active and covered the whole sky after ~1000 UT after the occurrence of another substorm (AE ~ 400 nT) at roughly 0930 UT. Some parts of the patches pulsated with periods less than a few seconds, while other parts did not. The whole structures drifted eastward with varying velocities. The patches are characterized by the green color, indicating auroral 557.7 nm emission. The orange emissions in the eastern and western edges of the images are reflection from city lights.

[7] The images in Figure 2 were taken with a zenith-pointing narrow FoV high-resolution CCD camera (body,

[1]Solar-Terrestrial Environment Laboratory, Nagoya University, Nagoya, Japan.
[2]Department of Physics and Technology, University of Tromsø, Tromsø, Norway.
[3]Department of Physics and Astronomy, University of Calgary, Calgary, Alberta, Canada.

0148-0227/10/2009JA014273$09.00

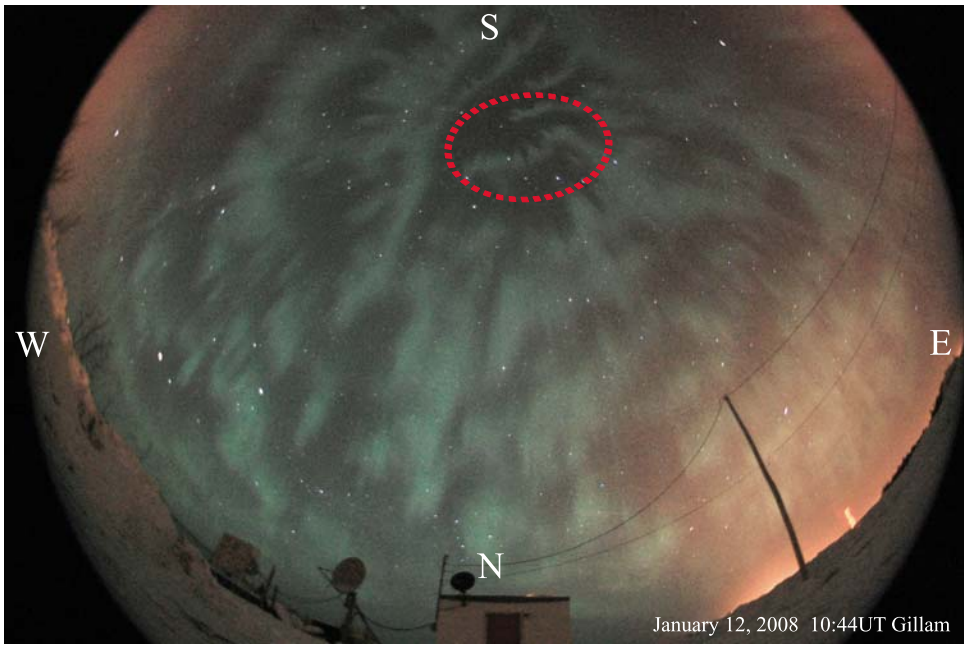

Figure 1. A photograph of auroral patches taken at 1044 UT (0425 LT) at Gillam, Canada. Camera, NIKON D40; lens, Nikon fish-eye 8 mm F2.8; exposure, 20 s; ISO setup, ISO800. The observatory hut is at the bottom of the photograph. The red circle indicates the patch structure focused in Figure 2.

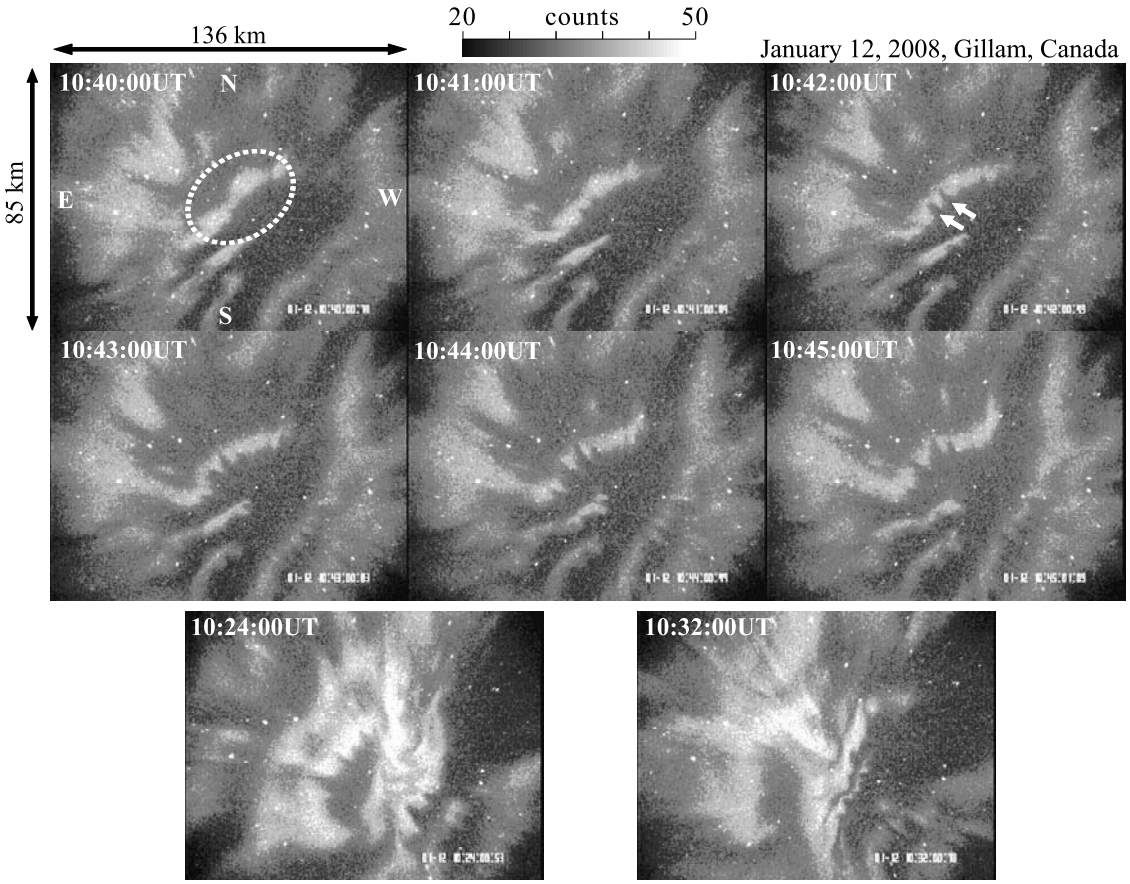

Figure 2. Panchromatic auroral images obtained with a narrow FoV CCD camera at Gillam, Canada, on 12 January 2008.

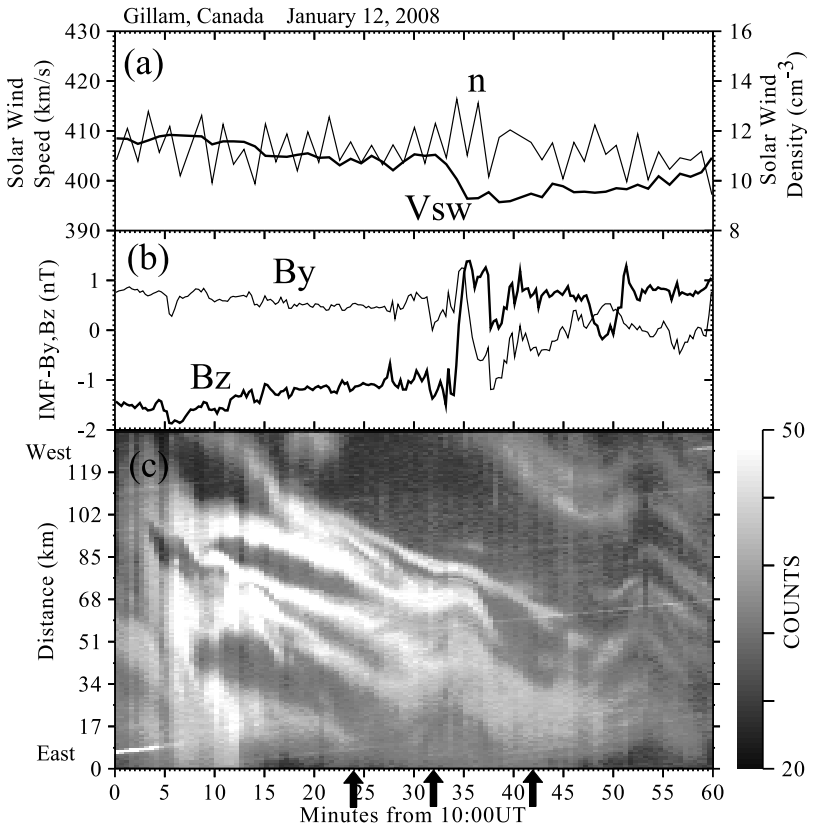

Figure 3. (a) Solar wind speed (thick line), density (thin line), and (b) IMF By and Bz, which are obtained with the ACE satellite at (217.6, 5.7, 22.4) R_E in GSM coordinates, and (c) east-west cross sections of auroral images obtained with a narrow FoV camera at Gillam at 1000–1100 UT (0341–0441 LT) on 12 January 2008. The ACE data were shifted by 56.3 min (= 217.6 R_E/411 km/s) by assuming average solar wind speed (411 km/s) during the plotted interval. The arrows indicate the timings when the finger-like structures shown in Figure 2 were observed.

WATEC WAT-120N+; lens, FUJINON DV10X7B-2) which was focused on the patch indicated by the red circle near the zenith in Figure 1. The camera is sensitive to the visible wavelengths. These images were taken with an exposure time of 1.07 s (32 video frames). The FoV of the camera is 48.5° × 35.3°. By assuming an altitude of 120 km for the 557.7 nm auroral emission, this FoV corresponds to an area of 136 km × 85 km. In the top six images (sequential images, every 1 min), the southwestern boundary of the patch structure highlighted with the white circle shows the development of finger-like dark structures during the period between 1040:00 UT and 1045:00 UT. The finger-like dark bands invade the patch from the southwest, as indicated by the white arrows. The scale size (wavelength) of the structure is ~5 km at an assumed emission altitude of 120 km. Similar invasion of finger-like dark structures into the patches and undulations of the western boundary of the patches were evident around 1000–1100 UT, as shown in the bottom two images. For both images, the dark finger-like structures invade the patches from the west.

[8] Figure 3c represents the east-west cross section of the images in Figure 2 for 1000–1100 UT (0341–0441 LT) and shows the longitudinal motion of the patch structures. The auroral structures move eastward at an average speed of ~30 m/s (= 50 km/30 min) for the plotted interval, most probably due to the background plasma convection in the morning sector. However, the convection velocity is not stable, and the auroral structures move back to the west at ~1030 UT and ~1050 UT. These changes seem to correspond to the northward turnings of IMF Bz, as shown in Figure 3b. These IMF and solar wind data were obtained with the ACE satellite at (217.6, 5.7, 22.4) R_E, and were shifted by 56.3 min (= 217.6 R_E/411 km/s) by assuming an average solar wind speed (411 km/s) during the plotted interval. It is noteworthy that the auroral convection speed responds to the northward turnings of IMF Bz almost instantaneously, with a time difference of less than 10 min. The black arrows indicate the timings when the finger-like structures in Figure 2 were observed in the images. Interestingly, they correspond to the timings when the convection slows down or turns westward.

[9] Animation 1 is compiled from the images used in Figures 2 and 3 for 1000–1100 UT every 30 s.[1] The fluctuation of the convection speed is clearly recognizable in Animation 1. The finger-like structures shown in Figure 2 develop when the convection slows down or turns westward. It is also noteworthy that several larger-scale finger-like dark structures with a width of ~20–50 km stretch over more than 100 km from northwest during the interval

[1] Animations are available in the HTML.

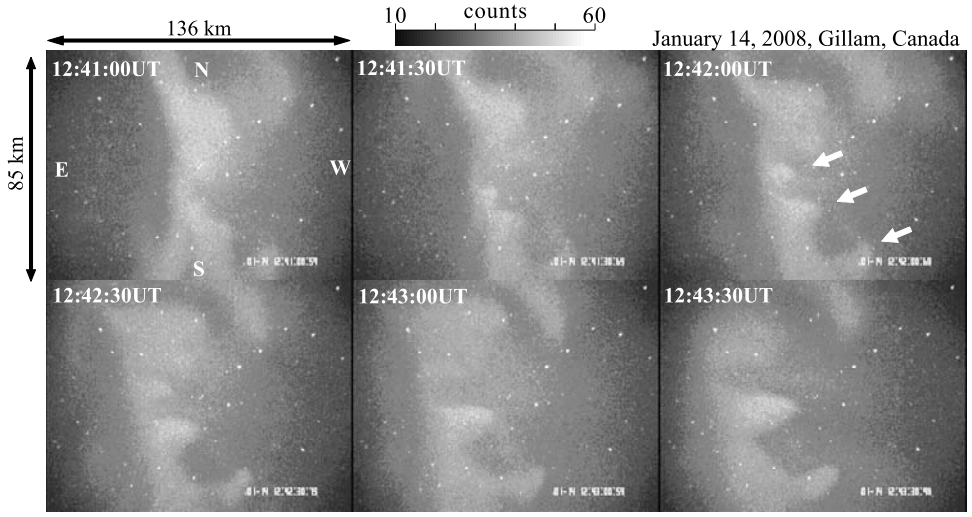

Figure 4. Panchromatic auroral images obtained at 1241:00–1243:30 UT (every 30 s) at Gillam, Canada, on 14 January 2008 in the same format as those in Figure 2.

between 1000 UT (at the northwestern edge of the image) and 1020 UT (over the eastern half of the image).

[10] Figure 4 shows another example of the finger-like structures at the western boundary of the patches, which was observed at 1241:00–1243:30 UT (~0633 LT) at Gillam on 14 January 2008 after an intense substorm around ~1100 UT (AE ~ 1500 nT). In this case, the finger-like bright structures develop at the western boundary of the patches, as indicated by the white arrows, while the whole structure drifts eastward relative to the ground at a speed of ~300 m/s. The north-south width of the structure was ~25 km, again assuming a 120 km emission altitude. The finger-like structures drift northward at a velocity of ~100 m/s. The southernmost finger-like bright structure became faint at 1241:31 UT and 1242:30 UT due to pulsation.

3. Summary and Discussion

[11] Using a narrow FoV camera in the auroral zone at Gillam (MLAT: 65.5°N), we observed finger-like structures with a scale size of 5–25 km at the western boundary of auroral patches in the postmidnight sector during substorm recovery phase on 12 and 14 January 2008. Both dark and bright finger-like structures were observed. The patches move eastward at speeds of ~30 m/s (12 January event) and ~300 m/s (14 January event), probably due to convection of background plasma. The finger-like structures seem to appear when the convection slows down.

[12] Figures 5a, 5b, and 5c are schematic illustrations of a possible mechanism for the generation of the observed finger-like structures at the western boundary of the auroral patches. Figure 5a shows a global view of the equatorial plane of the magnetosphere (top view from above the north pole). The observations in Figures 1–4 were made in the local time sector between midnight and dawn during the substorm recovery phase. For example, the field line from Gillam at 1030 UT on 12 January 2008 maps to the inner magnetosphere at X_{gsm} = −3 Re, Y_{gsm} = −6 Re using Tsyganenko-96 magnetic field model. Due to the substorm, hot plasma was injected into the midnight local time sector. The plasma in the postmidnight local time sector drifts eastward (sunward) due to the magnetic tension force and the large-scale pressure gradient force from the midnight sector, as indicated by the white arrow.

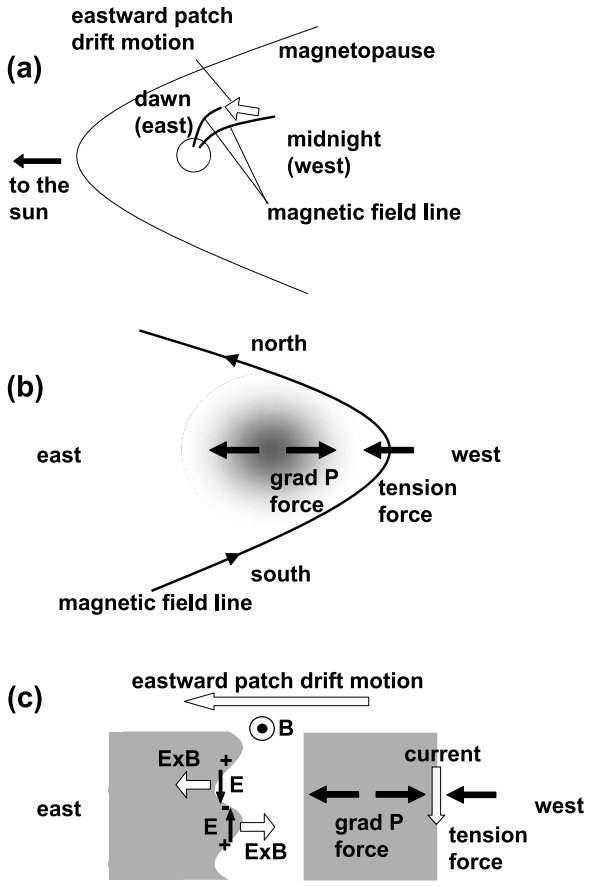

Figure 5. Schematic illustrations of the physical processes which cause the observed finger-like structures in the auroral patches: (a) global view, (b) local source region, and (c) top view of Figure 5b.

[13] Figure 5b shows a local source region of an auroral patch in the magnetosphere in the postmidnight sector (side view from dusk to dawn). We assume that the source region of the bright auroral patch is the region of high plasma pressure (either high plasma density or high temperature), as indicated by the shaded area. The direction of the local pressure gradient force is outward from the center of the patch. At the western boundary of the patch, this westward pressure gradient force balances with the magnetic tension force, which has an eastward (sunward) component in the postmidnight sector in addition to the earthward component since the magnetic field line is elongated tailward.

[14] Figure 5c is the top view of this local force balance in the equatorial plane of the magnetosphere (also in the ionosphere projected as auroral patches along the geomagnetic field line). At the surface of the force balance, electric current flows perpendicularly to the ambient magnetic field due to the pressure gradient and the curvature of the magnetic field. The Rayleigh-Taylor type instability can develop at the surface of this region of force balance. Namely, small perturbations at the surface result in the generation of polarization electric fields **E**, which makes the perturbation amplitude larger due to the **E** × **B** drift, causing finger-like structures to appear at the western boundary of the high-pressure region. This explains why the finger-like structures tend to occur in the western edge of the surface.

[15] The westward **E** × **B** drift causes brighter auroral structures developing to the west, and the eastward **E** × **B** drift causes darker auroral structures developing to the east. These instability developments occur at the region of most intense current density. This may cause the difference why the darker structure develops during the 12 January event (Figure 2) and brighter structure develops during the 14 January event (Figure 4).

[16] One can argue that this instability structure at the western edge of the high pressure region in the magnetosphere can be mapped to the poleward (northern) edge of the auroral patches in the ionosphere if the dipolar configuration of the geomagnetic field is taken into consideration. However, if the magnetospheric apex points of magnetic field lines from lower and higher ionospheric latitudes tend to align in the GSM-Y direction in the magnetosphere, the observed preference for the western side of the instability structure would occur. In Animation 1, several finger-like dark structures also develop from north to south at 1000–1020 UT, as noted in section 2.

[17] Strictly speaking, the term "Rayleigh-Taylor instability" should be used for the instabilities occurring at surfaces where there are gravitational forces at work. However, here we use this term to denote a similar instability, which is shown in Figure 5, by considering that the pressure gradient force and the centrifugal force due to the magnetic curvature are acting in place of the gravitational force. The instability in Figure 5 may be referred to as an interchange or flute instability [e.g., *Treumann and Baumjohann*, 1997] or pressure-driven instability. In any case, the observations presented in Figures 2 and 4 clearly indicate the existence of finger-like wave structures which suggest macroscopic instabilities at the western boundary of auroral patches. Since shear flow signatures parallel to the patch boundary were not observed for the present events, the finger-like structures were probably not caused by the Kelvin-Helmholtz type instability.

[18] The basic idea of similar macroscopic Rayleigh-Taylor type instability (ballooning and interchange instabilities) at the force balance surface between plasma pressure and magnetic tension has been considered in many previous studies [e.g., *Gold*, 1959; *Voronkov et al.*, 1997; *Cheng*, 2004; *Xing and Wolf*, 2007; *Kozlovsky et al.*, 2007; *Miura*, 2009], for larger-scale undulation of the magnetosphere at substorm onset and for the formation and modulation of auroral arcs. Further consideration would be necessary whether the observed small-scale (5–25 km) structures at the ionospheric altitude can map to the magnetosphere as a macroscopic Rayleigh-Taylor type instability. Considering the conservation of magnetic flux tube, the scale size of 5–25 km corresponds to the scale of ~200–1000 km at 10 Re in the magnetosphere, which is comparable or larger than the ion gyro radii in the inner plasma sheet.

[19] There has been an idea that the diffuse aurora is caused by pitch angle scattering of high-energy (~10 keV) electrons by electron cyclotron waves. Then the auroral patches can be a manifestation of ambient high-density low-energy plasma which causes the growth of the waves. If so, the pressure gradient at the boundary of auroral patches may not be significant to cause the pressure-driven instability proposed in this paper. Investigation of spatial structure of magnetospheric source plasma of auroral patches would be necessary in future, though mapping of the patches to the source magnetosphere is difficult.

[20] For the event of 12 January (Figures 2 and 3 and Animation 1), the instability seems to develop when the background drift slows down. The average speed of the eastward drift was very slow (~30 m/s = 1.7 mV/m) for the event of 12 January, and instability structures were frequently observed on this night. This fact might indicate that the background plasma convection works toward the stabilization of the instability, although the mechanism of the stabilization is not clear. The growth rate of this instability is expected to be larger for steeper pressure gradient at the patch boundary (i.e., when the perpendicular current is intense). The configuration in Figure 5b (the balance between the pressure gradient and the tension) prevails everywhere in the tail plasma sheet. Some type of stabilization mechanisms may occur to prevent the instability growth.

[21] The growth rate of Rayleigh-Taylor instability in plasma is given as $\gamma = (-g(n'/n))^{1/2}$ [e.g., *Chen*, 1974; *Treumann and Baumjohann*, 1997], where g is the acceleration of gravity, n is the plasma density, and $n' = \partial n/\partial z$ is spatial gradient of the density. Considering that the magnetic tension force, which is nearly equal to the pressure gradient force $P' = \partial P/\partial z$, works equivalent to the gravitational force, the growth rate γ becomes $(P'n'/n^2m)^{1/2}$. For $P' = 2$ nPa/Re, $n = 1$ cm^{-3}, $n' = 1$ cm^{-3}/Re, and $m = 1.67 \times 10^{-27}$ kg, the growth rate (e-folding time) becomes 6 s, which is fast enough to develop the observed instability structure. In the actual Earth's magnetosphere, however, the growth/suppression of the pressure-driven instability depends on various parameters, i.e., magnetic curvature, pressure gradient, plasma compressibility, plasma flow, and footprint ionospheric conductivity [e.g., *Ohtani and Tamao*, 1993]. The auroral patches are the most common feature in the diffuse auroral region. The instability reported in this paper divides larger-scale auroral source regions into smaller-scale structures.

Thus, this instability may be one of the causes that produce auroral patchy structures in the diffuse aurora.

[22] **Acknowledgments.** The observatories at Gillam and Fort Smith are Canadian Geospace Monitoring (CGSM) program core sites operated by the Canadian Space Agency. The campaign was carried out by the Solar-Terrestrial Environment Laboratory, Nagoya University, in collaboration with the Canadian Space Agency, and with support from the NORSTAR team of the University of Calgary. This work was supported by JSPS KAKENHI (19403010) and by Special Funds for Education and Research (Energy Transport Processes in Geospace) of the Ministry of Education, Culture, Sports, Science, and Technology of Japan.

[23] Amitava Bhattacharjee thanks Andrei Demekhov and another reviewer for their assistance in evaluating this paper.

References

Chen, F. F. (1974), *Introduction to Plasma Physics*, Plenum, New York.

Cheng, C. Z. (2004), Physics of substorm growth phase, onset, and dipolarization, *Space Sci. Rev.*, *113*, 207–270.

Gold, T. (1959), Motions in the magnetosphere of the Earth, *J. Geophys. Res.*, *64*(9), 1219–1224.

Goldstein, J., J. L. Burch, B. R. Sandel, S. B. Mende, P. C:son Brandt, and M. R. Hairston (2005), Coupled response of the inner magnetosphere and ionosphere on 17 April 2002, *J. Geophys. Res.*, *110*, A03205, doi:10.1029/2004JA010712.

Haerendel, G. (2007), Auroral arcs as sites of magnetic stress release, *J. Geophys. Res.*, *112*, A09214, doi:10.1029/2007JA012378.

Hallinan, T. J., and T. N. Davis (1970), Small-scale auroral arc distortions, *Planet. Space Sci.*, *18*, 1735–1744.

Kelley, M. C. (1986), Intense sheared flow as the origin of large-scale undulations of the edge of the diffuse aurora, *J. Geophys. Res.*, *91*, 3225–3230.

Kozlovsky, A., A. Aikio, T. Turunen, H. Nilsson, T. Sergienko, V. Safargaleev, and K. Kauristie (2007), Dynamics and electric currents of morningside Sun-aligned auroral arcs, *J. Geophys. Res.*, *112*, A06306, doi:10.1029/2006JA012244.

Lui, A. T. Y., C.-I. Meng, and S. Ismail (1982), Large amplitude undulations on the equatorial boundary of the diffuse aurora, *J. Geophys. Res.*, *87*, 2385–2400.

Mendillo, M., J. Baumgardner, and J. Providakes (1989), Ground-based imaging of detached arcs, ripples in the diffuse aurora, and patches of 6300-Å emission, *J. Geophys. Res.*, *94*, 5367–5381.

Miura, A. (2009), Pressure-driven and ionosphere-driven modes of magnetospheric interchange instability, *J. Geophys. Res.*, *114*, A02224, doi:10.1029/2008JA013663.

Nishitani, N., G. Hough, and M. W. J. Scourfield (1994), Spatial and temporal characteristics of giant undulations, *Geophys. Res. Lett.*, *21*(24), 2673–2676.

Ohtani, S.-I., and T. Tamao (1993), Does the ballooning instability trigger substorms in the near-Earth magnetotail?, *J. Geophys. Res.*, *98*(A11), 19,369–19,379.

Sandahl, I., T. Sergienko, and U. Brändström (2008), Fine structure of optical aurora, *J. Atmos. Sol. Terr. Phys.*, *70*, 2275–2292.

Semeter, J., and E. M. Blixt (2006), Evidence for Alfven wave dispersion identified in high-resolution auroral imagery, *Geophys. Res. Lett.*, *33*, L13106, doi:10.1029/2006GL026274.

Sergienko, T., I. Sandahl, B. Gustavsson, L. Andersson, U. Brändström, and Å. Steen (2008), A study of fine structure of diffuse aurora with ALIS-FAST measurements, *Ann. Geophys.*, *26*, 3185–3195.

Shiokawa, K., et al. (2009), Longitudinal development of a substorm brightening arc, *Ann. Geophys.*, *27*, 1935–1940.

Treumann, R. A., and W. Baumjohann (1997), *Advanced Space Plasma Physics*, Imperial Coll. Press, London.

Trondsen, T. S., and L. L. Cogger (1998), A survey of small-scale spatially periodic distortions of auroral forms, *J. Geophys. Res.*, *103*, 9405–9415.

Voronkov, I., R. Rankin, P. Frycz, V. T. Tikhonchuk, and J. C. Samson (1997), Coupling of shear flow and pressure gradient instabilities, *J. Geophys. Res.*, *102*, 9639–9650.

Xing, X., and R. A. Wolf (2007), Criterion for interchange instability in a plasma connected to a conducting ionosphere, *J. Geophys. Res.*, *112*, A12209, doi:10.1029/2007JA012535.

Yamamoto, T., K. Makita, and C.-I. Meng (1991), A particle simulation of large-amplitude undulations on the evening diffuse auroral boundary, *J. Geophys. Res.*, *96*(A2), 1439–1449.

Yamamoto, T., K. Makita, and C.-I. Meng (1993), A particle simulation of "giant" undulations on the evening diffuse auroral boundary, *J. Geophys. Res.*, *98*(A4), 5785–5800.

Zhang, Y., L. J. Paxton, D. Morrison, A. T. Y. Lui, H. Kil, B. Wolven, C.-I. Meng, and A. B. Christensen (2005), Undulations on the equatorward edge of the diffuse proton aurora: TIMED/GUVI observations, *J. Geophys. Res.*, *110*, A08211, doi:10.1029/2004JA010668.

T. Aslaksen, Department of Physics and Technology, University of Tromsø, N-9037 Tromsø, Norway. (torsten.aslaksen@gmail.com)

E. Donovan and M. Greffen, Department of Physics and Astronomy, University of Calgary, University Dr. NW, Calgary, AB T2N 1N4, Canada. (edonovan@ucalgary.ca)

A. Ieda, A. Nakajima, R. Nomura, K. Sakaguchi, and K. Shiokawa, Solar-Terrestrial Environment Laboratory, Nagoya University, Nagoya 464-8601, Japan. (shiokawa@stelab.nagoya-u.ac.jp)